Scientific
Research

CT Elastography: A Pilot Study via a New Endoscopic Tactile Sensor

Takehisa Sasaki, Mineyuki Haruta, Sadao Omata

NEWCAT Institute, Department of Electrical and Electronics Engineering, College of Engineering,
Nihon University, Koriyama, Japan
Email: take-cha@ee.ce.nihon-u.ac.jp

ABSTRACT

Objective: To develop a CT elastography imaging system useful for part of the human body in which ultrasound is not capable of reaching. The proposed system would measure CT modality through fusion of the stiffness mapping on the images by the tactile sensor system, improving precision of the endoscopic operation. Methods: We made some liver fibrosis phantoms of bovine skin gelatin with various densities as the target organ of the study. Using the tactile sensor system, which requires no compression during endoscopic operation, stiffness of each phantoms was measured. The resulting stiffness vs density curve was evaluated and translated to the stiffness vs CT number (Houndsfield Unit, HU) curve with a CT number vs density curve obtained by CT scan of the phantoms. A transformation formula can be deduced from these curves to the elasticity via CT number, which was confirmed *in vitro* with pig liver and *in vivo* CT scan data. Results: The stiffness and CT modality of each phantom was successfully measured and subjected to constant reduction. The CT value shows a linear relationship with the ROI values of the livers used. Conclusion: This paper reports method of supplementing stiffness information measured by a tactile sensor system, with a CT image for use with an endoscope. It is shown that CT number can be derived with a stiffness sensor and CT data in endoscopic surgery. From there results, we prove the possibility of measuring stiffness with CT and high resolution CT number.

KEYWORDS

1. Introduction

The stiffness of organs or tissues can be a possible index about a disease, the characteristic of the patient and an acute medical crisis or other dangerous states. Thus, the tissue elasticity is useful to confirm the diagnosis of disease, disordered function and evaluation of treatment. The need for pathological diagnosis or noninvasive screening is getting more and more importance these years. Malignancies such as cancers are known to be generally tense. By US elastography, we have been able to determine whether the stiffness of the lesion part was more firm compared to the neighboring organs. Some measurements of the stiffness of the living body and organ with a sensor system were previously reported for prostate [1,2], lymph lungs [3,4], myocardium [5], coronary arteries [6,7], breast

[8] and liver [9-12]. An endoscopic operation becomes more and more important as a low invasive surgery; in treatment, it is important that it allow grasping a puncture target and a puncture start position and a puncture course easily. In a surgical operation, the stiffness sensor with the small sense of touch sensor becomes important since tissue to remove surgically becomes smaller. In the case of liver elastgraphy, US echo elastgraphy is one of the most popular methods at present. The degree of fibrosis in the liver is known to be related to the stiffness of the liver, and the Fibroscan (Echosens, France) [9] and magnetic resonance elastography (MRE) [10], both of which evaluate liver fibrosis by the ultrasonic diagnosis have been developed. The principle of the FibroScan is based on US image analysis, which visualizes stiffness of organs according to measured differences in propagation

velocity of US pulse wave emitted to and reflected by liver. MRE system puts acoustic driver together to a MRI, which is a method to visualize local elastic modulus from wave motion images in tissue. Both systems can quantitatively measure elasticity and digitize the stiffness of liver in kPa, providing information on the progress of liver fibrosis. The principle of US echo elastography is real-time tissue elastography (RTE) and transient elastography (TE) for quantitative evaluation [11,12]. By comparing the signals of the target and checking objects, tumor and normal tissue can be qualitatively distinguished with regard to the measured stiffness. Each of the three methods, Fibroscan, MRE and US echo elastography mentioned above gives vibration from the outside and visualizes an elastic wave propagating the tissue, and can map the location and the volume of tumor by comparing the stiffness to the normal tissue. The main therapeutic methods for burning up liver cancer include percutaneous microwave coagulation therapy (PMCT) and radio-frequency ablation (RFA) [13,14]. In a surgical operation of PMCT and RFA, the puncture starting point and the path to the puncture target can be easily guided using a US echo mapped image [15,16]. At present endoscopic surgery mainly depends on US elastography imaging, however, CT image guided surgery was once performed in the past [17-19]. It is necessary to add a touch sensor in addition to a basic function to a forceps used for an endoscopic operation and laparoscopic surgery. The function to confirm the stiffness of tumor with a sense of touch sensor is important, however, it is still in the development stage and not yet suitable for practical use. As for other organs than the liver mentioned above, it is necessary to measure the stiffness of the part having difficulty in palpation and the deep part or the other side of the bone prior to the examination in screening and endoscope preparation. We examined the possibility of the CT elastography, which could noninvasively provide stiffness information fused on the CT image for various organs by taking differences in stiffness between the target objects and the standard objects of known stiffness. In this paper we report a method to obtain stiffness information via tactile sensor system developed for endoscope operation.

2. Materials and Methods

2.1. Define about a Coefficient of Elasticity: Young's Modulus

In the following manner, we defined an elasticity (Young) of the biological tissue. The unit is [kPa] same as the materials fixed number. We prepared known homogeneous standard materials beforehand. We measured it using a load sensor used in a road cell. We measured the elasticity of the known isotropic and homogeneous materials in kPa by a load sensor used in the road cell. The Young's modulus that is a modulus of elasticity is uni-

form for strength of materials and is the materials fixed number for the material with the isotropy. In other words, as for expressing hardness of biological tissue comprised of complicated materials as a Young's modulus, there is unreasonableness basically. Based upon the foregoing, each researcher wrote the hardness of the living body soft tissue using each measuring equipment originally conventionally and has been reported for a relative value. After 2000, as Natural SI Unit, it was suggested we standardized the hardness of the living body soft tissue using kPa and displayed it and to weigh it. Our definition and measurement of the elasticity follow those of R. M. Hochmuch *et al*. [20]. In other words, we define the hardness of the biological soft tissue which we should relatively compare as an absolutely needed quantity. Even this study and this article adopt this suggestion.

2.2. Liver Fibrosis Phantom

Make a twenty-one fibrosis phantoms of the 1.0% stepping fine from concentration of 1.0% to 7.0% from concentration using the bovine skin gelatin with pure water, and salt water. (**Figure 1(a)**) When CT scanning, in order to state close to a living body CT number of the fibrosis phantoms was created with salt water as a solvent, 2% and 4%. When CT scan sets into a cylinder type phantom, **Figure 1(b)** shows this cylinder phantom's geometry of concentration of gelatin (**Figure 1(c)**).

2.3. Tactile Sensor System

Show circuit diagram of tactile sensor system for endoscopic

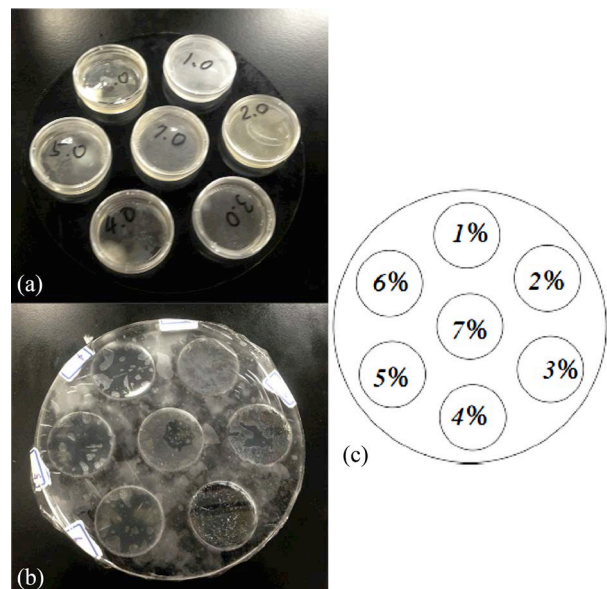(a)

(b)

(c)

1%
2%
6%
7%
3%
5%
4%

Figure 1. Liver fibrosis phantoms and cylinder type. (a) The fibrosis phantoms for stiffness sensor; (b) A cylinder type fibrosis phantom for CT scan; (c) A geometry of concentrations of gelatin in a cylinder phantom.

operations in **Figure 2(a)**, was developed by Omata *et al.* in 1995 [1]. A piezo sensor is attached to a tip of the probe tip coming in contact with a measurement object. The output signal from a piezo sensor is input into an amplifier and puts a signal amplified by an amplifier through the bandpass filter and returns in the bias of the piezo sensor after having passed a filter and constitutes feedback loop. piezo sensor after having passed a filter and constitutes feedback loop. **Figure 2(b)** shows a photograph of overview of tactile sensor system we have developed a sensor attached to the tip of endoscopes, constituted of a sensor probe with a piezo sensor, an amplifier, a bandpass filter (BPF) circuit, a frequency counter by microcontroller unit (MCU) and a PC. Show a photograph of tactile sensor system overview, it is a system with the load to the measurement subject object of the sensor as uniformity quantitatively to evaluate it. This experience system used to calibrate of tactile sensor system. We constituted a this measurement system in Labview to give the weighting of the fixed quantity to normal position (vertically) for an object targeted for a measurement by a sensor probe, labview calculates a coefficient of elasticity [kPa] from the output result of the sensor and records it to a PC [8]. The positioning with the motor to add weighting and the flow that I receive the output of the sensor and do are controlled in Labview, Labview performs the positioning with the motor to add weighting and receives the output of the sensor and constitutes a flow to carry out a calculation.

2.4. Method

Figure 3 shows the outline of the experiment. Elasticity was measured by the tactile sensor system in kPa at 11 points on the surface of each fibrosis phantoms. **Figure 3** [1] shows the measured elasticity as a function of density of gelatin. Cylinder type Fibrosis phantoms were concentrically set on the gantry bed of the CT and Scanned. From this measurement result, make a number of the coefficient of elasticity—concentration of gelatin graph. **Figure 3** [1], result is plot by boxplot of Gnuplot (GNU Fundation). Prepared a tray of acrylic to place the fibrosis phantoms concentrically for CT scan, put a tray with fibrosis phantoms on CT gantry bed, scanning the fibrosis phantoms. Calculate Standard Deviation: SD of Region of Interest: ROI in DICOM image of CT scan of each fibrosis phantom, make a number of the CT-number (Hounsfield Unit: HU)—concentration of gelatin graph. **Figure 3** [2] Make the graph of the coefficient of elasticity [kPa]—CT-number from a coefficient of elasticity [kPa] of graph **Figure 3** [1] and an CT-number of graph **Figure 3** [2] in a standard by Gelatin concentration, confirm correlation from this elasticity [kPa]—CT-number of graph.
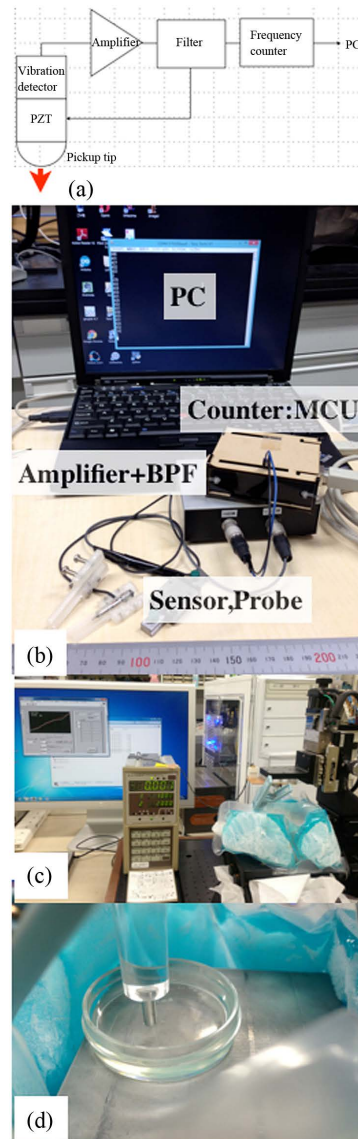

Figure 2. **Tactile sensor circuit, system and Experiment. (a) Circuit diagram of phase shift circuit; (b) Overview of a sensor system for Endoscopic operation; (c) Calibration system for tactile sensor by loadcell; (d) Sensing on surface of phantom.**

Figure 3 [3] regression line solve by Ordinary Least Squares method: OLS from this graph **Figure 3** [3], confirm R2 (R-squared, coefficient of determination), use software Gnuplot(GNU). Prepare an image as modality data to process, CT scan image data of liver and kidney of pig (1 yo, Male, wo/past illnesses control) of our CT data library show **Figure 3** [4]. Perform the following steps to get image of CT elastography. First, extracts the region of the liver from the CT data. Substitute expression-1 for this extracted the region of the liver, generate the file which convert CT-number (HU) reading into a coefficient of elasticity [kPa]. Display a formed this generated file in a color table, show sample of axicial image
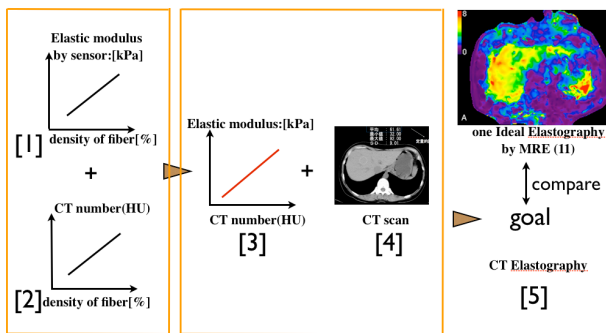
Figure 3. Experiment overview. [1] A graph of stiffness [kPa] —concentrations of bovine skin gelatin [%]; [2] A graph of CT-number—concentrations of bovine skin gelatin [%]; [3] A graph f stiffness [kPa]—CT-number; [4] CT scan data; [5] Make a histogram as a stiffness map, calculate by expression (1) and expression (2). And compare data *in vivo*.

Figure 3 [5] The next step is Volume Rendering work. Volume rendering work are segmented the region of the liver from the CT data, exclude and remove Hepatic Veins, Hepatic Arteries and Portal Veins from liver ROI [17,18]. Convert it here, CT-number reading into a coefficient of elasticity [kPa]. Extract ROI of the normal stiffness cell, calculate SD in ROI. Using intensity histogram and scroll bar, extract the cell which is harder than a normal cell's SD. Also extract the cell which is softer than a normal cell's SD. Display the cell which is harder than this normal or the softer than this normal cell at the same time, in other words, we get the volume rendering image which let you reflect stiffness ratio. And so measure with a hardness sensor for the organs of the pig *in vivo* and evaluate it. We use OsiriX (Ver 5.8 for MacOSX) and ImageJ (1.46 r, NIH) with plug-in Interactive 3D Surface Plot (k.barthel, Internationale Medieninformatik, Germany) for calculation of SD of ROI and stiffness mapping, and use to make a graph by Gnuplot (ver.4.6.3, GNU). The translated using the constant expression mentioned above a number of the histogram to create a stiffness-mapping. CT scanner is Shimadu Sabrina SCT-7800, scan condition 120 kV/130 mAs, Helical pitch 5 mm, slice 5 mm. e output of the sensor and constitutes a flow to carry out a calculation.

2.5. Pig Liver *in Vitro*

We used the liver of pig food, which is commercially available. And put any acrylic markers on the peritoneum over liver and kidney before CT scan of the pig **Figure 4**. And measure the abdominal pressure of pig. This is to measure the stiffness and CT number at the same point. After CT scan, measure stiffness of the same point.

2.6. CT Number of Phantoms

After CT scan of cylinder phantom, measure CT number

and calculation by ImageJ. The DICOM image file check by Osirix. of the same point **Figure 5**.

3. Result

3.1. Elastsgraphy of Liver Fibrosis Phantom

The results of measurement of elasticity for each fibrosis phantoms by tactile sensor system were shown in **Table 1**. Show graph of SD of coefficient of elasticity—concentration of gelatin (**Table 1**).

$$y(\text{kPa}) = 10.625x(\%) + 2.035, \ R^2 = 0.9819 \qquad (1)$$

3.2. CT Number of Fibrosis Phantom

CT scan of Liver fibrosis phantom, the results of measurement of CT-number for each fibrosis phantoms by

Figure 4. Acrylic marker on surface of pig liver sample.

Figure 5. A cylinder phantom, confirmed HU and SD.

Table 1. Stiffness—concentrations of brovine skin gelatin.

Concentrations of gelatin [%]	3%	4%	5%	6%	7%
	38.8	43.3	61.8	56.5	88.5
Stiffness [kPa]	33.6	43.8	56.9	69.8	83.1
(Young's modulus)	35.5	42.9	53.7	62.2	83.7
n = 11	37.4	42.7	58.8	75.7	77.0
	36.6	41.8	56.0	68.4	72.5
	37.9	42.7	54.2	63.1	78.5
	32.8	43.6	50.9	63.2	76.1
	38.4	43.1	51.1	67.4	73.6
	38.8	39.9	52.0	65.5	72.9
	36.6	42.4	50.7	61.4	75.8
	30.3	41.8	51.0	61.2	76.5
Average (mean)	**36.1**	**42.5**	**54.3**	**64.9**	**78.0**
Standard Deviation	**2.8**	**1.1**	**3.7**	**5.2**	**5.1**

CT scanner were shown in **Table 2**. Show graph of SD of coefficient of CT number—concentration of gelatin (**Tables 2**). A regression line of each sodium chloride solution 2.0% and 4.0% is

$$y(HU) = 1.896x(\%) + 31.34 \, (NaCl \, 2.0\%) \quad (2a)$$

$$y(HU) = 2.028x(\%) + 55.25 \, (NaCl \, 4.0\%) \quad (2b)$$

3.3. Equations: Elastgraphy and CT-Number

Made the graph of the coefficient of elasticity [kPa]—CT-number from a coefficient of elasticity [kPa] of graph **Figure 6** and an CT-number of graph **Figure 7** in a standard by Gelatin density, confirm correlation from this elasticity [kPa]—CT-number of graph. **Figure 8** Calculate regression line solve by Ordinary Least Squares method: OLS from this graph **Figure 6**, linear equations. Thus, expression (3a), (3b) from expression (1) and expression (2a), (2b),

$$y(kPa) = 5.23x(HU) - 286.88 \, (NaCl \, 2\%) \quad (3a)$$

$$y(kPa) = 10.625x(HU) + 2.035 \, (NaCl \, 4\%) \quad (3b)$$

Substitute this expression (3b) up to (3a) for each pixel value of ROI of liver.

3.4. ROI of CT Image to Stiffness Map

Show CT scan data. **Figure 9(a)** The stiffness value of each pixel value of ROI of the pig liver using the transformation formula of linear form, before exchange to stiffness mapping, the fixed expression (3a) is substituted for this CT number after this and is calculated. **Figure 9(b)** The stiffness-mapped CT image was obtained by calculating stiffness of each pixel value of ROI of the pig's liver using the transformation formula of linear form.

Table 2. Stiffness—concentrations of bovine skin gelatin, 2% and 4% of salt (NaCl) concentration.

Gelatin [%]	0%		1.0%		2.0%		3.0%	
NaCl: 2%	HU	SD	HU	SD	HU	SD	HU	SD
	28.4	12.7	31.5	9.2	35.5	10.2	37.8	13.4
	35.6	14.4	32.0	11.6	34.5	11.1	38.3	13.7
	32.4	12.9	32.1	12.7	34.0	11.2	38.1	14.3
	29.3	10.9	31.3	11.7	34.8	10.1	38.5	13.1
Mean	31.4	12.7	31.7	11.3	34.7	10.7	38.2	13.6
Gelatin [%]	4.0%		5.0%		6.0%		7.0%	
NaCl: 2%	38.2	10.7	40.6	10.9	39.5	11.8	44.1	9.4
	37.7	12.7	41.5	11.1	43.4	13.6	44.7	9.6
	37.3	11.8	41.1	12.1	43.6	14.7	44.4	11.2
	38.6	11.1	40.9	11.2	43.4	15.0	43.7	11.2
Mean	38.0	11.6	41.0	11.3	42.5	13.8	44.2	10.3
Gelatin [%]	0%		1.0%		2.0%		3.0%	
NaCl: 4%	51.2	16.5	59.0	11.9	61.3	14.3	63.5	16.8
	55.6	12.9	57.5	12.9	60.5	12.9	63.5	16.9
	52.2	16.4	57.2	12.8	60.4	13.1	63.1	17.3
	53.3	15.9	58.6	12.7	61.0	12.3	63.2	17.3
Mean	53.1	15.4	58.1	12.6	60.8	13.1	63.3	17.1
Gelatin [%]	4.0%		5.0%		6.0%		7.0%	
NaCl: 4%	63.6	12.0	66.6	14.4	67.9	17.5	69.2	12.6
	62.5	13.5	65.2	14.1	67.0	18.6	68.1	14.7
	63.7	13.1	66.2	13.7	68.0	17.9	68.2	14.7
	64.6	14.4	66.2	13.5	69.9	14.9	67.5	17.7
Mean	63.6	13.3	66.0	13.9	68.2	17.2	68.3	14.9
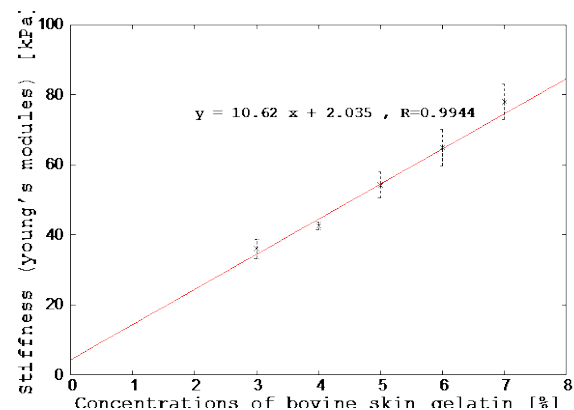
Figure 6. Stiffness—concentration of gelatin.
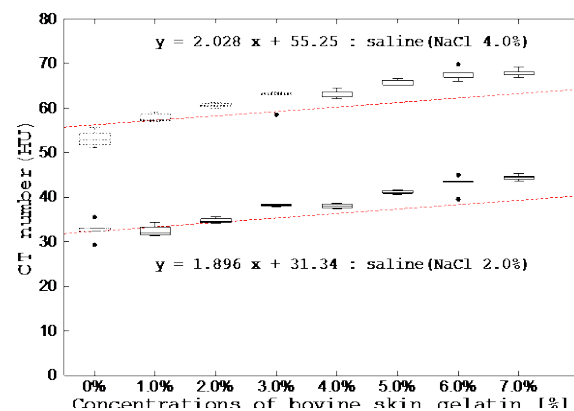
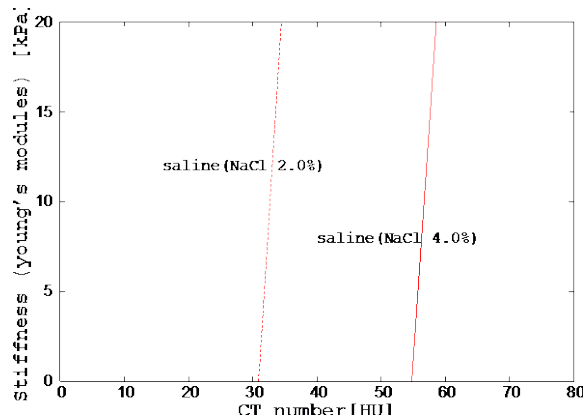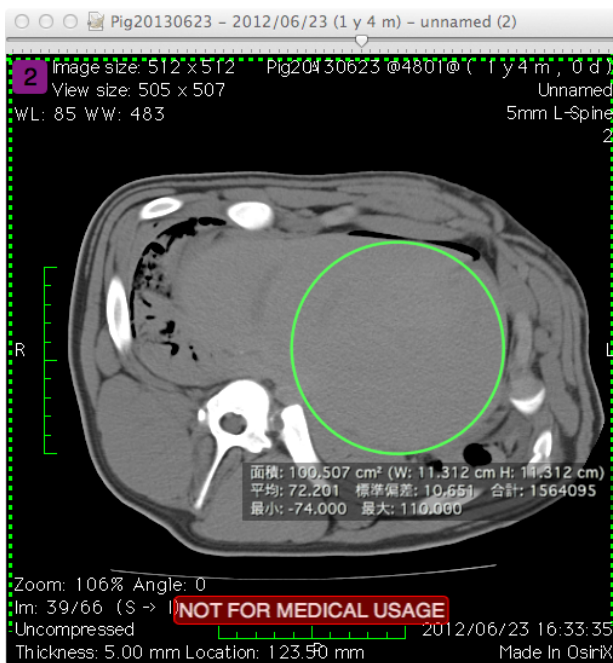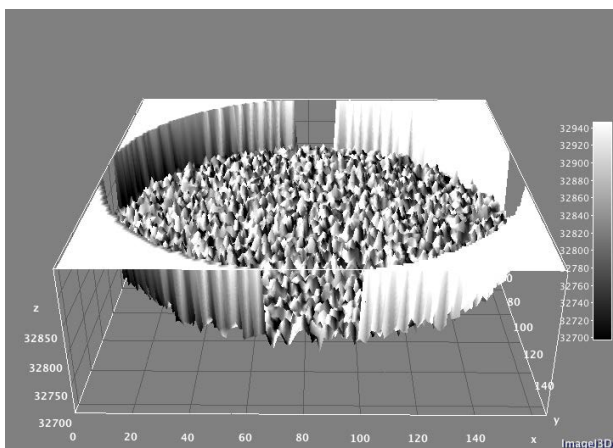**Figure 7. CT number—concentration of gelatin.**

Figure 8. Stiffness—CT number(HU).

(a)

(b)

Figure 9. (a) ROI of CT image of pig liver; (b) A histogram before as a stiffness mapping of ROI by expression (3b).

3.5. Calibration of CT Scanner

About resolution of our CT scanner, when start scan, calibration by water phantom, diameter is R = 225 mm. **Figure 10**. The ROI (square, 40 pixel) are arranged on the circumference of a circle consisting of a diameter "R/2" at regular intervals respectively. **Table 3** is measured CT number in ROI.

4. Conclusion

In this paper we report on a CT elastographic imaging method, which provides stiffness information for the CT modality by transforming CT number to the tissue stiffness using a tactile sensor for the endoscopic operation. And the CT number for fat is not considered, because it has a negative value. About fatty liver and non-alcoholic steatohepatitis (NASH), they will be included in the next paper. CT elastography is quite possible provided that CT number of the ROI on the target organ and stiffness of the reference organ are available. The CT images can be converted to stiffness mapped images using the relationship between the CT number and the tissue stiffness once the stiffness of the surface of a normal liver was obtained by a tactile sensor attached to the head of a probe, and that is how the sense of touch plays a key role in improving tumor identification in the CT guided endoscopic tumor resection. In another paper we will report on an application of this method to some clinical cases.
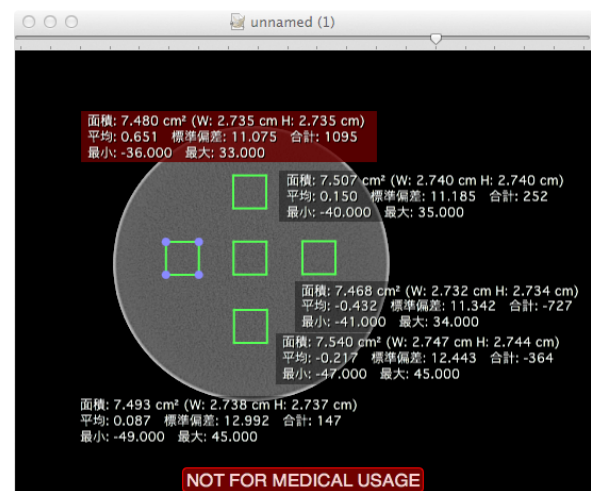

Figure 10. Water phantom of CT scan for calibration, calculated by Osirix5.8.

Table 3. CT scan of water phantom.

ROI#	1	2	3	4	5	Ave
HU:Ave	1.37	1.18	1.14	1.03	0.95	1.13
SD	10.78	10.70	10.75	10.80	10.83	10.77
max	48	53	48	46	48	49
min	−59	−50	−51	−50	−54	−54

Acknowledgements

REFERENCES

[1] O. Sadao and C. E. Constantinou, "Constantinou Modeling of Micturition Characteristics Based on Prostatic Stiffness Modulation Induced Using Hormones and Adrenergic Antagonists," *IEEE Transactions on Biomedical Engineering*, Vol. 42, No. 8, 1995, pp. 843-848. http://dx.doi.org/10.1109/10.398646

[2] V. Jalkanen, B. M. Andersson, A. Bergh, *et al*., "Prostate Tissue Stiffness as Measured with a Resonance Sensor System: A Study on Silicone and Human Prostate Tissue *in Vitro*," *Medical and Biological Engineering and Computing*, Vol. 44, No. 7, 2006, pp. 593-603. http://dx.doi.org/10.1007/s11517-006-0069-6

[3] K. Miyaji, A. Furuse, J. Nakajima, *et al*., "The Stiffness of Lymph Nodes Containing Lung Carcinoma Metastases: a New Diagnostic Parameter Measured by a Tactile Sensor," *Cancer*, Vol. 40, No. 8, 1995, pp. 1432-1436.

[4] T. Ohtsuka, A. Furuse, T. Kohno, *et al*., "Application of a New Tactile Sensor to Thoracoscopic Surgery: Experimental and Clinical Study," *The Annals of Thoracic Surgery*, Vol. 60, No. 3, 1995, pp. 610-614. http://dx.doi.org/10.1016/0003-4975(95)00483-2

[5] M. K. Sugiura, S. Omata, S. Kaneko, *et al*., "Clinical and Biochemical Spectrum of Zinc Deficiency in Human Subjects," *Journal of the American College of Cardiology*, Vol. 31 No. 5, 1998, pp. 1165-1173. http://dx.doi.org/10.1016/S0735-1097(98)00063-1

[6] L. Wexler, B. Brundage, *et al*., "Coronary Artery Calcification: Pathophysiology, Epidemiology, Imaging Methods, and Clinical Implications," *Circulation*, Vol. 94, 1996, No. 5, pp. 1175-1192. http://dx.doi.org/10.1161/01.CIR.94.5.1175

[7] A. S. Agatston, W. R. Janowitz, *et al*., "Quantification of Coronary Artery Calcium Using Ultrafast Computed Tomography," *Journal of the American College of Cardiology*, Vol. 15, No. 4, 1990, pp. 827-832.

[8] S. Omata and Y. Terunuma, "New Tactile Sensor Like the Human Hand and Its Applications," *Sensors and Actuators*, Vol. 35, No. 1, 1992, pp. 9-15. http://dx.doi.org/10.1016/0924-4247(92)87002-X

[9] L. Sandrin, C. Fournier, *et al*., "Fibroscan® in Hepatology: A Clinically-Validated Tool Using Vibration-Controlled Transient Elastography," 2009 *IEEE International Ultrasonics Symposium*, Rome, 20-23 September 2009, pp. 1431-1434.

[10] R. Muthupillai, D. J. Lomas, P. J. Rossman, *et al*., "Magnetic Resonance Elastography by Direct Visualization of Propagating Acoustic Strain Waves," *Science*, Vol. 269, No. 5232, 1995, pp. 1854-1857.

[11] U. Motosugi, *et al*., "Effects of Gadoxetic Acid on Liver Elasticity Measurement by Using Magnetic Resonance Elastography," *Magnetic Resonance Imaging*, Vol. 30, No. 1, 2012, pp. 128-132. http://dx.doi.org/10.1016/j.mri.2011.08.005

[12] E. Ueno, E. Tohno, *et al*., "Dynamic Tests in Real-Time Breast Echography," *Ultrasound in Medicine & Biology*, Vol. 14, Supplement 1, 1988, pp. 53-57. http://dx.doi.org/10.1016/0301-5629(88)90047-6

[13] A. Itoh, *et al*., "Breast Disease: Clinical Application of US Elastography for Diagnosis," *Radiology*, Vol. 239, No. 2, 2006, pp. 341-350.

[14] T. Seki, *et al*., "Ultrasonically Guided Percutaneous Microwave Coagulation Therapy for Small Hepatic Cancer," *Cancer*, Vol. 74, No. 3, 1994, pp. 817-825. http://dx.doi.org/10.1002/1097-0142(19940801)74:3<817::AID-CNCR2820740306>3.0.CO;2-8

[15] S. Rossi, M. Di Stasi, *et al*., "Percutaneous RF Interstitial Thermal Ablation in the Treatment of Small Hepatic Cancer," *Journal of the American College of Cardiology*, Vol. 167, 1996, pp. 759-768.

[16] S. Rossi, F. Fornari and L. Buscarini, "Percutaneous Ultrasound-Guided Radiofrequency Electrocautery for the Treatment of Small Hepatocellular Carcinoma," *Journal of Vascular and Interventional Radiology*, Vol. 8, 1993, pp. 97-103.

[17] C. Kubisch, S. Glaßer, *et al*., "Vessel Visualization with Volume Rendering," *Visualization in Medicine and Life Sciences II Mathematics and Visualization*, Springer, Berlin, Heidelberg, 2012, pp. 109-132. http://dx.doi.org/10.1007/978-3-642-21608-4_7

[18] B. B. Frericks, F. C. Caldarone and B. Nashan, "3D CT Modeling of Hepatic Vessel Architecture and Volume Calculation in Living Donated Liver Transplantation," *European Radiology*, Vol. 14, No. 2, 2004, pp. 326-333.

[19] J. D. Stefansic, A. J. Herline, Y. Shyr, *et al*., "Registration of Physical Space to Laparoscopic Image Space for Use in Minimally Invasive Hepatic Surgery," *IEEE Transactions on Medical Imaging*, Vol. 19, No. 10, 2000, pp. 1012-1023. http://dx.doi.org/10.1109/42.887616

[20] R. M. Hochmuch, "Micropipette Aspiration of Living Cells," *Journal of Biomechanics*, Vol. 33, No. 1, 2000, pp. 15-25.